Publisher version DOI: 10.1109/TCST.2020.3006123

An LPV approach to Autonomous Vehicle Path Tracking in the Presence of Steering Actuation Nonlinearities

Matteo Corno[a], Giulio Panzani[a], Federico Roselli[a], Michele Giorelli[b], Davide Azzolini[b] and Sergio M. Savaresi[a]

Abstract—**The paper deals with trajectory tracking for autonomous cars during evasive manoeuvres and in the presence of steering actuator nonlinearities. The paper develops an LPV MISO H-infinty controller based on the feedback of the lateral error at the centre of gravity and at the look-ahead distance. The controller architecture offers a way to cope with the effect of the steering nonlinearities, by scheduling one of the control weighting functions. A detailed experimental validation on three different manoeuvres (straight driving, wide bend and a double lane change) shows the effectiveness of the proposed LPV solution.**

I. INTRODUCTION

The escalation towards higher levels of road vehicle autonomy is one of the main drivers of automotive research and is also heavily shaping the automotive industry. From the control point of view, most autonomous driving systems are categorized around two main subsystems: path planning and path tracking [1]. The former module, using environmental sensors and information, determines the desired path in global coordinates: this is an extremely rich and lively research field with many contributions, see for example [2]–[4]. The latter, the path tracking controller, acts on the vehicle actuators (steering, throttle, and braking) to track the reference path. This is usually achieved using inertial measurement and position information that can be obtained fusing GPS, cameras and other sensors. Two independent levels usually manages the path tracking task: a longitudinal controller (*i.e.* reference speed tracking) and lateral controller (*i.e.* reference path tracking).

Since the 1980s, when technology made it realistic, vehicle path tracking and in particular the lateral control problem has received thorough scientific scrutiny. The literature on this topic is vast. A great variety of control paradigms have been applied: among the most successful sliding mode control [5], non-linear control [6], [7], Potential field control [8]–[10], Model Predictive Control [11]–[14], and Optimal Preview control [15], [16] can be listed. Beside the different approaches, the literature agrees on some points: the benefits introduced by a feedforward/preview term [17], the need of including the vehicle speed in the lateral control design and that some level of look-ahead is essential (guaranteed by the access to the future planned path of the high-level controller) to provide accurate path tracking.

Regardless of the approach, the steer-by-wire actuator has a large impact on the path tracking controller: actuator dynamics, friction and backlash limit the achievable performance. Not many publications explicitly account for this; notable exceptions are the experimental works by Gerdes' group [18] where the steer-by-wire system is modelled as a second order system. However, the group employed a high performing steer-by-wire system which does not seem to use off-the-shelf components. The other relevant work in this direction is [19]: in this case the steer nonlinearities are treated as a bounded disturbance which is considered in the design of a linear controller.

This paper focuses on path tracking in the case of evasive manoeuvres and high speed-driving; in particular, we design a Linear Parameter Varying controller [20], [21] that achieves safe and efficient path tracking. The proposed strategy originates from the approach firstly introduced in [22], that reformulates the problem as the control of two variables: the lateral error at the vehicle centre of gravity (CoG) and the derivative of the look-ahead error. Such approach combines a rather simple controller structure with interesting tracking performance. In short summary, its relevance is the use of future information (provided by a look-ahead contribution) in a genuine feedback fashion (opposite to feed-forward approaches, which usually suffer the robustness issue), without the need of running online optimizations (that would be required by *e.g.* an MPC approach); moreover, the resulting Multiple Input Single Output (MISO) controller is systematically designed by means of an H-infinty approach.

Unfortunately, the proposed controller does not address two important issues. The first one is that the variation of the vehicle speed is not taken into account in the controller design. The second is related to the performance of the low-level steering controller that highly influences the closed-loop performance and driving comfort; this second aspect is usually underestimated by the scientific literature but is expected to become increasingly important, given the maturity of the autonomous driving field.

In summary, this work extends the lateral controller [22] introducing gain scheduling. Such choice offers a way to systematically include two scheduling variables in the controller: the vehicle speed, which naturally appears in the vehicle dynamics model, and the road curvature, that helps to mitigate the effect of the steering actuator nonlinearities on the driving comfort. On the other side, the LPV extension doesn't alter the original controller structure preserving its discussed advantages. The controller extensions and design discussion is supported by simulation results and experiment tests on a test track with standard and dynamic manoeuvres close to the handling limits.

II. EXPERIMENTAL SET-UP

All the results presented in the paper refer to the vehicle shown in Figure 1, a production Dodge Dart which has been retrofitted. Its main parameters are listed in Table I.

For the control of the longitudinal dynamics, the vehicle is equipped with a *Throttle-by-wire* and a *Brake-by-wire* system: the former, which is standard issue in the production vehicle, is controlled by overriding the command sent to the ECU; the latter

[a] M. Corno, G. Panzani, F. Roselli and S. Savaresi are with Dipartimento di Elettronica Informazione e Bioingegneria at Politecnico di Milano. matteo.corno@polimi.it, giulio.panzani@polimi.it, federico.roselli@polimi.it, sergio.savaresi@polimi.it

[b] Michele Giorelli and Davide Azzolini are with Technology Innovation, Automated Driving Technologies, Magneti Marelli, Viale Carlo Emanuele II, 150, 10078 Venaria Reale TO. michele.giorelli@magnetimarelli.com, davide.azzolini@magnetimarelli.com

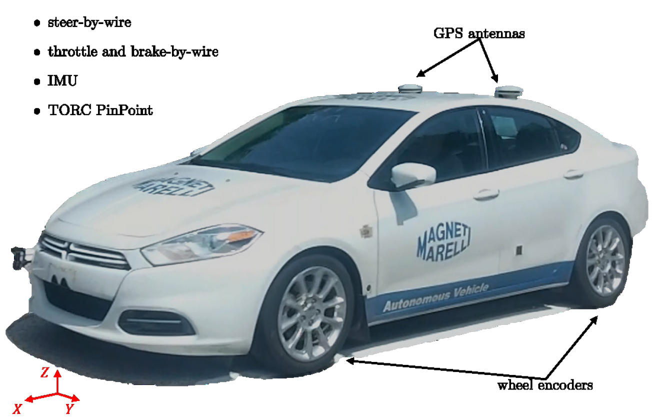

Fig. 1. The autonomous vehicle employed in this work.

is achieved by means of a linear actuator directly pushing the brake pedal. In order to enable the autonomous trajectory tracking a *Steer-by-wire* system is installed: it is composed of an electric motor connected to the standard steering column through a belt transmission. The steering angle is controlled by a third-party proprietary control system. The steering system, with its relevant nonlinearities, represents the limit of today's cost-effective technology and addressing such limitation is an often underrated issue in literature.

The vehicle is also equipped with the following sensors: an Inertial Measurement Unit that provides the linear accelerations (longitudinal and lateral), four wheels speed sensors and a TORC Robotics PinPoint Localization and Precision IMU [23] that provides inertial measurements and, through sensor fusion, the position of the vehicle with an accuracy of 0.01m at a rate of 100Hz.

Regarding the autonomous driving control architecture, it is assumed that a high level path planner provides the desired trajectory in global coordinates. Moreover, to ease the discussion, we further assume that the longitudinal speed control problem is solved and that the vehicle proceeds at the desired velocity.

III. MODELLING

This section recalls and validates the main control oriented models employed in the remainder of the paper. Following a bottom-up approach, we present the actuator, the vehicle dynamics and the trajectory tracking model.

TABLE I
VEHICLE PARAMETERS.

Parameter	Symbol	Value	Unit
Mass	M	1895	Kg
Wheelbase	L	2.703	m
Front axle-CoG distance	l_f	1.177	m
Steering ratio	n_{st0}	1/14.54	-
Wheel radius	R_w	0.31	m
Yaw inertia	J_z	2400	kgm^2
Front cornering stiffness	C_f	124900	N/rad
Rear cornering stiffness	C_r	166000	N/rad

A. Steer-by-Wire model

It is a common practice, in the development of complex vehicle dynamics systems, to have several control layers: among the lowest, the actuator one is usually responsible for the sole control of the actuators. Its main objective is to guarantee a repeatable, with small steady-state error, and linear response of the actuator. A good actuator control needs to be robust to friction, backlashes, plays and saturations that characterize the actuator. Whereas the first two goals can be usually achieved by a proper application of standard linear control techniques, *e.g.* PD controllers [18], the last objective is more challenging especially when changes of system parameters – due for example to ageing and wearing – have to be accounted for. In this case, traditional control strategies yield repeatable, with small steady-state error, but mostly nonlinear responses; the nonlinearities are better addressed by more complex control structures *e.g.* [24].

As denoted in Section II, a low-level proprietary controller is responsible for the position control of the steering column. In order to build a simulation/control oriented model, we use a grey-box approach. Figure 2 shows the main elements we consider the in model. It features: a delay that accounts for the typical communication protocols between the central processing unit and the actuator driver; a position controller, modelled as a PID; a second order linear dynamic block that represents the mechanical dynamics of the steering column and finally a nonlinear Stribeck [25] friction block that accounts for the main nonlinearity.

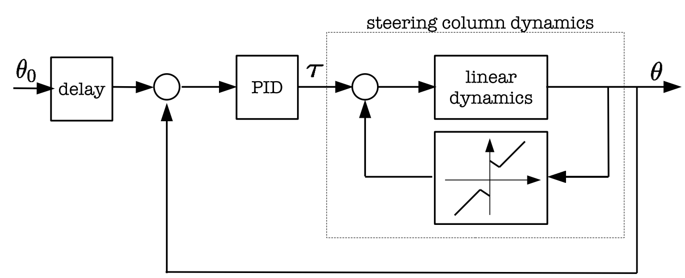

Fig. 2. Functional description of the Steer-by-wire model.

Given the limited knowledge of the actuation system, all the model's parameters are identified through grey-box optimization. Two types of experiments are considered: a 10° amplitude sinusoidal oscillation, used to better characterize the stick-slip phenomena that arise because of the friction, and faster steps to assess the linear response when the friction is negligible compared to the inertial effects. Figure 3 shows the comparison between the modelled steering wheel position and the measured one. The inspection of the experimental results validates the effectiveness of the proposed steering system model, both for small and large excitations. Form the analysis, it is clear that the steering dynamics cannot be neglected: while for slow actuations the nonlinear static effects are more prominent, with evident stick-slip phenomena, for rapid actuation the response is quite accurately described by a second order delayed linear response.

B. Vehicle dynamics

The vehicle lateral dynamics are described by the classical single-track model [26], that assumes small steering angles, a path radius

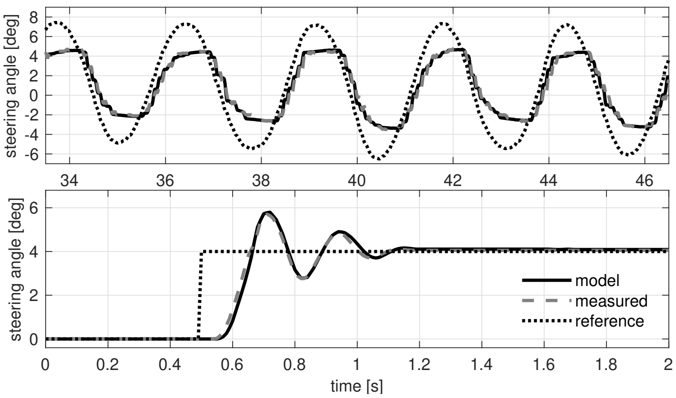

Fig. 3. Validation of the actuator model for slowly (top) and fast (bottom) varying steering angles.

larger than the wheelbase, slowly-varying speed and linear tire characteristic. The model results in the following state-space equations:

$$\begin{aligned} \dot{V}_y &= -\frac{C_f+C_r}{Mv}V_y+\left(\frac{C_r l_r - C_f l_f}{Mv}-v\right)r+\frac{C_f}{M}\delta_w \\ \dot{r} &= \frac{C_r l_r - C_f l_f}{J_z}\beta-\frac{C_f l_f^2+C_r l_r^2}{J_z v}r+\frac{C_f l_f}{J_z}\delta_w \end{aligned} \tag{1}$$

where v is the velocity, r is the yaw rate, V_y is the lateral component of the velocity vector, C_f and C_r are respectively the front and rear cornering stiffness, J_z is the total yaw inertia of the vehicle, l_f and l_r are the distances between the CoG and the front and rear axle and δ_w is the steering angle at the wheels.

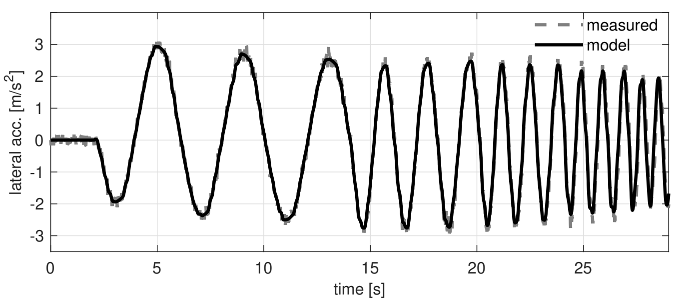

Fig. 4. Vehicle model validation with a steering sweep test at 70 km/h.

Figure 4 plots the validation of the model from the lateral acceleration point of view: the experiment is performed at 70 km/h with a sweep on the steering wheel, manually performed by the driver to exclude the nonlinear effects of the steer-by-wire system.

C. Trajectory Tracking model

The Trajectory Tracking model describes the evolution of the vehicle position with respect to the target path. The latter is well described by the reference path curvature ρ_{ref} whereas the former is well characterized by means of the tracking error at the CoG, e_{cg}. Moreover, given its importance in the literature ([27], [28]) the look-ahead error e_{la} is also introduced (as depicted in Figure 5). Assuming a small angular difference ($\Delta\psi$) between the vehicle heading and the track yaw, the rate of change of the lateral error is computed as

$$\dot{e}_{cg} = v(\beta+\Delta\psi) \tag{2}$$

with

$$\Delta\dot{\psi} = r-\rho_t v. \tag{3}$$

Similarly, the state equation for the look-ahead error is

$$\dot{e}_{la} = \dot{e}_{cg}+d_{la}\Delta\dot{\psi} = v(\beta+\Delta\psi)+d_{la}(r-\rho_{ref}v). \tag{4}$$

The vehicle and the path tracking dynamics (1)-(4) are summarized in the compact form (5).

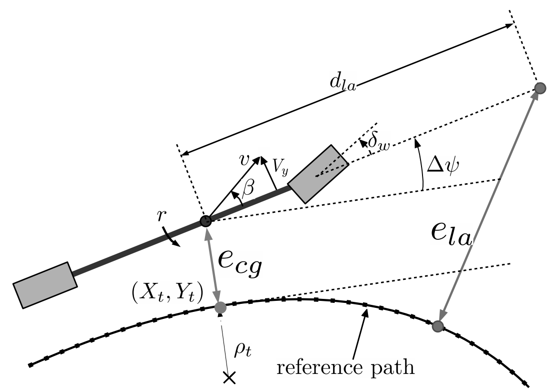

Fig. 5. Lateral error and look-ahead error definition.

The overall system is Multiple Input Multiple Output, where the inputs are the controllable steering angle and the known reference curvature (computed at the nearest point on the reference path). The CoG error is one output of the system; additionally, also the time derivative of the error at the look-ahead distance is included as a controller output.

The look-ahead distance d_{la} and the vehicle speed v can be considered parameters: the former is a tuning parameter, whereas the latter is a measurable time-varying one.

IV. LPV PATH TRACKING CONTROL

A. Controller description

As discussed in the introduction, the present work extends [22], where a linear H-infinity path tracking controller is based on the feedback of two variables: the lateral tracking error and the derivative of the look-ahead one. In spite of its simplicity, the controller shows excellent tracking performance on real autonomous driving tests.

Unfortunately, it does not address two important issues. The first one is related to vehicle speed that, as shown in Section III, influences the tracking dynamics. This is a known issue and it is widely accepted that in order to achieve the adequate level of performance, especially for dynamic manoeuvres, the vehicle speed must be taken into account.

The second issue is related to the behaviour of the low-level steering controller. Indeed, the original controller assumes that all the involved dynamics are linear, including the actuator ones. However, Section III shows that the linear model is valid only when the steering is actuated with sufficiently high speed, but when the steering rates are low, friction nonlinearities play an important role. It is therefore expected that during, for example, straight driving, the closed-loop performance will not match the design specifications. To better catch the relevance of the actuator nonlinearities on the vehicle tracking behaviour, Figure 6 depicts the results of a closed-loop (using the discussed controller [22]) simulation during straight driving

$$
\begin{bmatrix} \dot{V}_y \\ \dot{r} \\ \Delta\dot{\psi} \\ \dot{e}_{cg} \end{bmatrix} = \begin{bmatrix} -\frac{C_f+C_r}{Mv} & \frac{C_r l_r - C_f l_f}{Mv} - v & 0 & 0 \\ \frac{C_r l_r - C_f l_f}{J_z v} & -\frac{C_f l_f^2 + C_r l_r^2}{J_z v} & 0 & 0 \\ 0 & 1 & 0 & 0 \\ 1 & 0 & v & 0 \end{bmatrix} \begin{bmatrix} V_y \\ r \\ \Delta\psi \\ e_{cg} \end{bmatrix} + \begin{bmatrix} \frac{C_f}{M} & 0 \\ \frac{C_f l_f}{J_z} & 0 \\ 0 & -v \\ 0 & 0 \end{bmatrix} \begin{bmatrix} \delta_w \\ \rho_{ref} \end{bmatrix}
$$

$$
\begin{bmatrix} y_1 \\ y_2 \end{bmatrix} = \begin{bmatrix} 0 & 0 & 0 & 1 \\ 1 & d_{la} & v & 0 \end{bmatrix} \begin{bmatrix} V_y \\ r \\ \Delta\psi \\ e_{cg} \end{bmatrix} + \begin{bmatrix} 0 & 0 \\ 0 & -d_{la} v \end{bmatrix} \begin{bmatrix} \delta_w \\ \rho_{ref} \end{bmatrix} \tag{5}
$$

with and without the inclusion of the actuator frictions. In the linear case, as expected, the response settles to null tracking error, and the steering angle to zero. When friction is included, the system exhibits a limit cycle where the error and the steer continue to oscillate. As further validation, real data from an analogous experiment are added to the plot for comparison: notice that being a closed-loop test the time domain trajectories are different but the amplitude and the frequency of the oscillations resemble and validate the simulated ones.

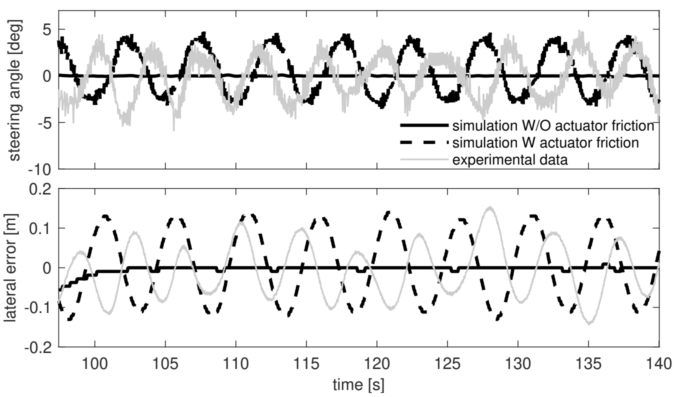

Fig. 6. Effect of the actuator nonlinearities on the driving performances.

The LPV framework can address both issues. In fact, the controller is an output feedback controller whose parameters are automatically "gain-scheduled" according to the time-varying values assumed by a set of parameters $p(t)$. In the LPV framework, it is described by the following equations:

$$
\begin{cases} \dot{\zeta} = A_k(p)\zeta + B_k(p)y \\ u = C_k(p)\zeta + D_k(p)y \end{cases} \tag{6}
$$

where the system matrices linearly depend on the polytopic coordinates (marked with Π_i):

$$
\begin{bmatrix} A_k(p) & B_k(p) \\ C_k(p) & D_k(p) \end{bmatrix} = \sum_{i=1}^{q} \alpha_i(p) \begin{bmatrix} A_k(\Pi_i) & B_k(\Pi_i) \\ C_k(\Pi_i) & D_k(\Pi_i) \end{bmatrix}. \tag{7}
$$

The LPV controller can be designed to ensure closed-loop stability and to minimize a quadratic $\mathcal{H}_\infty$ performance by solving a system of Linear Matrix Inequalities (see [29] for further details). This can be done if the controlled system dynamics can be expressed as an LPV plant and providing possibly parameter dependent (see [30]) dynamic weights, that define the desired performances.

The block diagram of overall control scheme, meant for the H-infinity control design, is represented in Figure 7. It features (from left to right): the controller $K(s,p)$, the linear steering-actuator

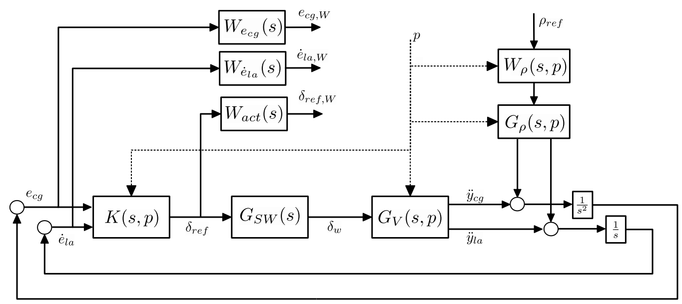

Fig. 7. LPV closed-Loop control scheme of the combined CoG and Look-Ahead strategy.

dynamics augmented with a Pade' approximation of the delay $G_{SW}(s)$, the vehicle and trajectory tracking model $G_V(s,p)$ and the effect of the reference path curvature $G_\rho(s,p)$ on CoG error.

Five dynamic weights are introduced to shape the closed-loop properties of the controlled system:

- $W_{e_{cg}}(s)$ shapes the *closed-loop sensitivity* referred to the lateral error e_{cg};
- $W_{\dot{e}_{la}}(s)$ shapes the *closed-loop sensitivity* referred to the Look-Ahead error derivative $\dot{e}_{la}$;
- $W_{act}(s)$ shapes the *control effort sensitivity*. Its main objective is to avoid high frequency actuation that the steer-by-wire would not be able to track;
- $W_\rho(s,p)$ weighs the effect of the disturbance in the loop; it is chosen as a first order filter replicating the maximum frequency content of an aggressive manoeuvre.

Compared with the control scheme previously proposed in [22], consistently with the LPV framework some components of the block diagram are now dependent on the parameters vector p (time dependency has been omitted for simplicity): the self-scheduled controller $K(s,p)$, but also the system dynamics $G_V(s,p)$, $G_\rho(s,p)$ and the weighting function $W_\rho(s,p)$. The selected time-varying parameters p are related to the vehicle speed and the target path curvature: they are precisely introduced in the next sections.

1) Velocity scheduling: the influence of the vehicle speed is recast in the LPV framework by inspecting the system equations (5). Despite the system matrices are not linearly dependent on the longitudinal speed a convenient, albeit conservative, affine description of the system is possible considering v and $\frac{1}{v}$ as two independent parameters. Within this perspective, the vehicle and trajectory tracking dynamics can be written as a combination of 3 matrices

$$\begin{aligned}\dot{x} &= \left(A_0 + A_1\frac{1}{v} + A_2 v\right)x + \left(B_0 + B_1\frac{1}{v} + B_2 v\right)u \\ y &= \left(C_0 + C_1\frac{1}{v} + C_2 v\right)x + \left(D_0 + D_1\frac{1}{v} + D_2 v\right)u\end{aligned} \tag{8}$$

where

$$\begin{aligned}
A_0 &= \begin{bmatrix} 0 & 0 & 0 & 0 \\ 0 & 0 & 0 & 0 \\ 0 & 1 & 0 & 0 \\ 1 & 0 & 0 & 0 \end{bmatrix} \qquad A_2 = \begin{bmatrix} 0 & -1 & 0 & 0 \\ 0 & 0 & 0 & 0 \\ 0 & 0 & 0 & 0 \\ 0 & 0 & 1 & 0 \end{bmatrix} \\
A_1 &= \begin{bmatrix} -\frac{C_r + C_f}{M} & \frac{C_r l_r - C_f l_f}{M} & 0 & 0 \\ \frac{C_r l_r - C_f l_f}{J_z} & -\frac{C_r l_r^2 + C_f l_f^2}{J_z} & 0 & 0 \\ 0 & 0 & 0 & 0 \\ 0 & 0 & 0 & 0 \end{bmatrix} \\
B_0 &= \begin{bmatrix} \frac{C_f}{M} & 0 \\ \frac{C_f l_f}{J_z} & 0 \\ 0 & 0 \\ 0 & 0 \end{bmatrix} \qquad B_1 = \underline{0} \quad B_2 = \begin{bmatrix} 0 & 0 \\ 0 & 0 \\ 0 & 1 \\ 0 & 0 \end{bmatrix} \\
C_0 &= \begin{bmatrix} 0 & 0 & 0 & 1 \\ 1 & d_{la} & 0 & 0 \end{bmatrix} \qquad C_1 = \underline{0} \quad C_2 = \begin{bmatrix} 0 & 0 & 0 & 0 \\ 0 & 0 & 1 & 0 \end{bmatrix} \\
D_0 &= \underline{0} \qquad D_1 = \underline{0} \quad D_2 = \begin{bmatrix} 0 & 0 \\ 0 & -d_{la} \end{bmatrix}
\end{aligned} \tag{9}$$

This description of the controller dynamics allows one to easily include the velocity effect in the LPV controller, by means of the LMI design [29]. Additionally, to reduce the conservativeness coming from the use of two non-independent parameters, their dependence is in fact exploited describing the parameter space with a 3 vertexes polytope (opposite to the 4 vertex polytope standardly used for truly independent parameters): see Figure 8. It is interesting

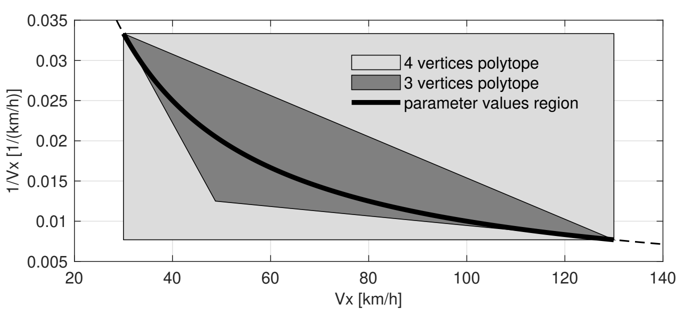

Fig. 8. Polytopes for the velocity parameter space description. The black line is the curve of the possible values assumed by the (not independent) parameters.

to note that, in view of the classical two independent controllers architecture (lateral and longitudinal), the path tracking controller will be exposed to relatively slow variations of velocity during aggressive maneuvers. In fact, it is common practice to decouple the braking (or acceleration) and steering phases of an evasive maneuvers.

2) Curvature Scheduling: a cost-effective control-based solution is here proposed to cope with the undesired effects induced by the servo-controller nonlinearities shown in Figure 6, still preserving the linear controller structure. Such solution is based on the evidence that the properties of the limit cycle induced by the steer-by-wire actuator are significantly affected by the trajectory tracking control bandwidth. Its effects are summarized by the experimental results presented in Figure 9 (also supported by simulations, here omitted for the sake of conciseness), where the spectra of the lateral acceleration and the tracking error at the centre of gravity are shown for a straight run experiment at 85 km/h, with different control bandwidths. The

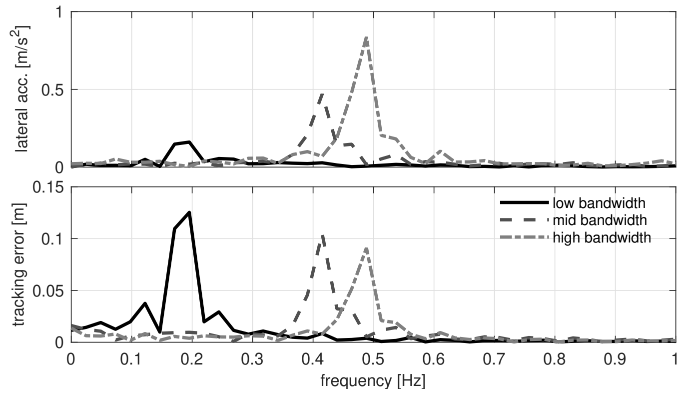

Fig. 9. Spectra of the lateral acceleration and tracking error obtained during a 20 second experiment at 85 km/h.

controller bandwidth has an impact on the tracking error but, more interestingly, on the perceived driving comfort here represented with the lateral acceleration. In particular, for a high bandwidth controller not only the acceleration values increase, but mainly focus around 0.5 Hz, a frequency at which passengers are particularly sensitive. Opposite the lowest bandwidth yields a slightly larger tracking error (still below 15 cm) but a considerable reduction in both the amplitude and frequency of the lateral acceleration. This analysis proves that a different controller tuning can improve comfort with a limited effect on tracking performance during straight driving.

Unfortunately, detuning the controller during transient and cornering manoeuvres leads to unacceptable tracking errors. This is shown in Figure 10 where a wide bend with a constant radius of 70 m is performed varying the controller bandwidth: the tracking error reaches values of around 1 m for the lowest tuning.

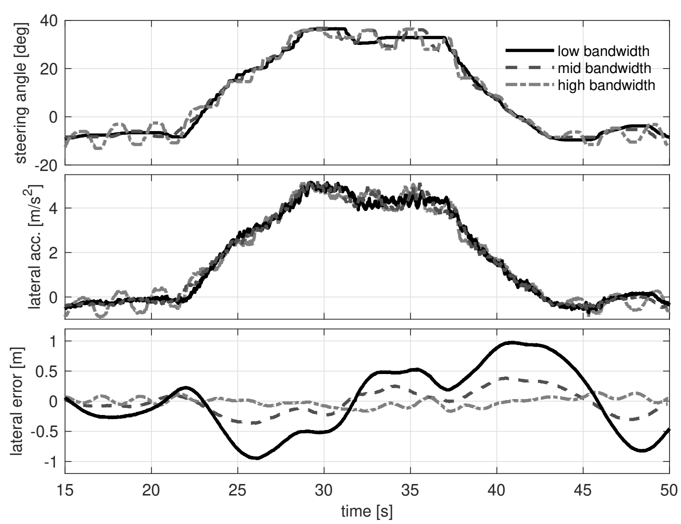

Fig. 10. Steering angle and tracking error for a wide bend at 70 km/h

Unexpectedly, a trade-off arises: the lateral errors reached for the de-tuned case are compatible with rectilinear driving requirements, but do not guarantee a safe execution of transient and cornering manoeuvres. To systematically solve this trade-off, the proposed solution is to modify the controller bandwidth depending on whether the vehicle is negotiating a corner or not. An additional scheduling implements this idea: the weighting functions $W_\rho(s,p)$, is adapted according to the variation of a parameter α, that indicates whether the vehicle is cornering or not; in particular, $W_\rho(s,p)$ is designed so that its pole frequency is reduced when straight driving is ongoing. Acting on the weighting functions $W_\rho(s,p)$ rather than on the more intuitive $W_{e_{cg}}(s)$ and $W_{\dot{e}_{la}}(s)$ helps to reduce the tuning efforts, still yielding the desired bandwidth modification. In fact, lowering the bandwidth of $W_\rho(s,p)$ implies that the effect of a disturbance (the curvature, as in Figure 7) is considered less important at higher frequency, leading to a less reactive (*i.e.* with lower bandwidth) controller.

A good candidate for the parameter α could be the reference curvature. However, if only the current curvature were considered the controller would be affected by a delay, *i.e.* the vehicle would start negotiating aggressive manoeuvres with a tuning close designed for straight driving. Thus, the actual scheduling parameter α is computed linearly remapping the path curvature ρ_{ref} into the variable $\tilde{\rho}_{ref} \in [0,1]$ so that $\rho_{ref,min} = 0$, $\rho_{ref,max} = 1$ and saturating the result.

$$\alpha(t) = \mathrm{sat}_{[0,1]}(\tilde{\rho}_{ref}). \tag{10}$$

Values of α must be interpreted so that 0 refers to straight driving and 1 to turning. In order to reduce the effect of noise and outliers in the target path definition, the reference curvature is averaged in the time window $t \in [-T_{past}, T_{preview}]$ before computing $\tilde{\rho}_{ref}$, taking advantage of the future values of the reference trajectory.

The reference path curvature scheduling is the central idea that makes the proposed approach different from [19] which is, to the best of author's knowledge, the only work that explicitly considers a non-ideal steer-by-wire in the control design. Beside minor differences in the context (*e.g.* the mentioned work does not explicitly address the autonomous path tracking problem but refers to a generic longitudinal speed - yaw rate control problem) the most important one is how authors treat the steer backlash hysteresis: as a bounded disturbance linearly entering the plant and including its effect in a performance norm minimization problem. In our approach, in fact, we opt for a varying importance of the effect of the steer nonlinearities, depending on the type of reference trajectory and we modify the controller tuning accordingly.

In conclusion, referring to the overall control architecture of Figure 7 the parameter vector $p(t)$ is

$$p = \begin{bmatrix} \frac{1}{v}, & v, & \alpha \end{bmatrix}$$

and the number of vertices q in equation (7) results equal to 6.

V. EXPERIMENTAL VALIDATION

A. Controller tuning

In the following, we validate the controller in different scenarios on the instrumented vehicle. Table II lists the values of controller parameters.

The parameters tuning has been performed sequentially

1. Tuning of the weighting functions, with look-ahead distance of 9 m (consistent with from previous scientific literature, *e.g* [17]).

TABLE II
CONTROLLER PARAMETERS

$W_{e_{cg}} = \frac{0.01s+0.632}{s+0.0632}$	$W_{\dot{e}_{la}} = \frac{0.99s+0.267}{s+0.0267}$
$W_{act} = \frac{s+130}{s+1441}$	$d_{la} = 12$ [m]
$W_\rho = 0.02\frac{1+s/(2\pi 100 f_\rho)}{1+s/(2\pi f_\rho)}$	$f_\rho = 0.0475\alpha + 0.0025$ [Hz]

2. Tuning of the Look-ahead distance.
3. Design and curvature scheduling of $W_\rho(s,\alpha)$; notice that the speed scheduling is naturally "embedded" in the LPV structure of the controlled plant and does not require any further tuning.

Even if the sequential tuning does not offer any guarantee of optimality, simulations and experimental tuning always led to tracking performance increase at each step, yielding to overall satisfactory results.

Regarding the weighting functions, a pole/zero structure has been found sufficient to achieve satisfactory results. $W_{\dot{e}_{la}}(s)$ dominates at higher frequencies compared to $W_{e_{cg}}(s)$, given its "prediction" role within the control law. Consistently with the low-level position in the control law hierarchy, the actuator weighting function has the highest bandwidth.

The look-ahead tuning optimizes the following trade-off: for short look-ahead distances the vehicle reacts too late when changes in the target trajectory occur; too long distances cause the vehicle to anticipate the manoeuvre and "cutting corners". The proposed value averages the experimental results on different manoeuvres.

Finally, the curvature scheduling is obtained by changing the pole/zero frequency of $W_\rho(s,\alpha)$, namely f_ρ (see Table II) according to the curvature (through the parameter α, see (10)). Firstly fixed values of f_ρ are found to yield the desired performance during straight driving and cornering: for the former a value of $f_\rho = 0.0025$ Hz is found (corresponding to the "Low bandwidth" case of Figure 9), and for the latter a value of $f_\rho = 0.05$ Hz (the "High bandwidth" case of Figure 10). The scheduling is then obtained with a linear transition between these two values, as function of the parameter α.

B. Results

The proposed controller is tested against two different scenarios. The first one is the track shown in Figure 11 that features two wide bends and connecting straights, mainly meant to verify the effect of the curvature scheduling and the overall performances. Figure

Fig. 11. Autonomous driving test track.

12 shows one full lap at 80 km/h proving how the curvature based

scheduling improves the oscillations on the straight sections without deteriorating the cornering capabilities. The figure shows two sets

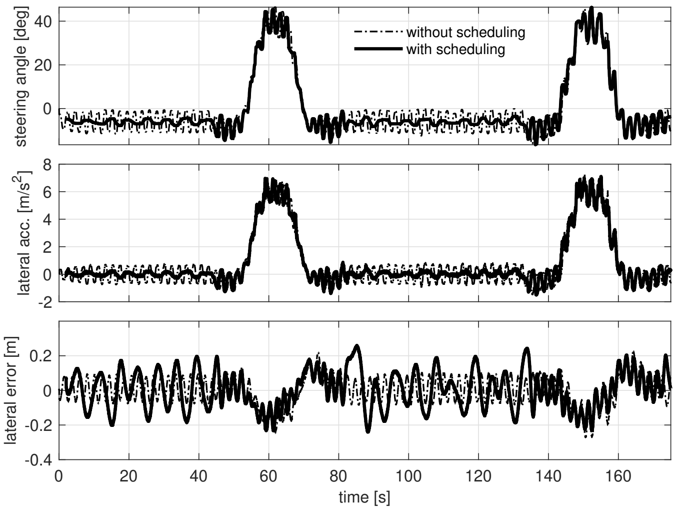

Fig. 12. Comparison between the fully (velocity and curvature) scheduled controller and the velocity only scheduled controller.

of data: a test in which only the velocity scheduling is active, and a second test in which the full scheduling is used. As expected, based on the discussion of Section IV, one can see that the full scheduling yields an accurate tracking of the trajectory during cornering and a comfortable straight driving with limited lateral acceleration. The transition phase from straight driving to cornering is detailed in Figure 13: in particular the bottom plot shows the scheduling variable α, the scaled path curvature and the average one. The use of future – available – target trajectory values effectively includes an equivalent a-causal filtered curvature signal where noise has been cleaned out without introducing time delays. Notice that in this experiment the transition phase is relatively rapid and well managed by the scheduling: the employed LPV approach ensures the stability of the closed-loop system.

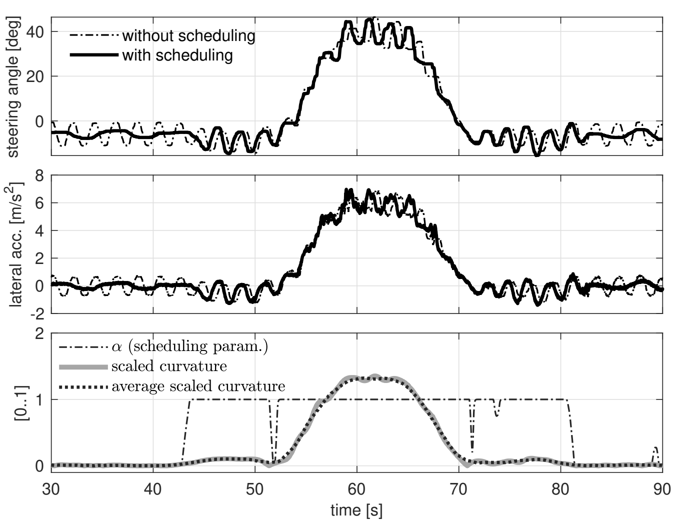

Fig. 13. Details on the transition phase from straight to cornering.

The second manoeuvre is the Double Lane Change (DLC) performed at different speed (ranging from 50 to 90 km/h), meant to validate the controller performances for highly dynamic manoeuvres. Figure 14 compares the simulated and the experimental results in terms of tracking root mean squared error at different speed (maximum lateral accelerations are also provided in the right plots for a better experiment contextualization) which, when the LPV controller is used, keeps almost constant and limited to satisfactory values. To better appreciate the effect of the speed scheduling, the DLC manoeuvre is also simulated for a fixed controller tuning (at a nominal speed of 70km/h) yielding to higher and more variable rms values. To show the good performance achieved with the proposed

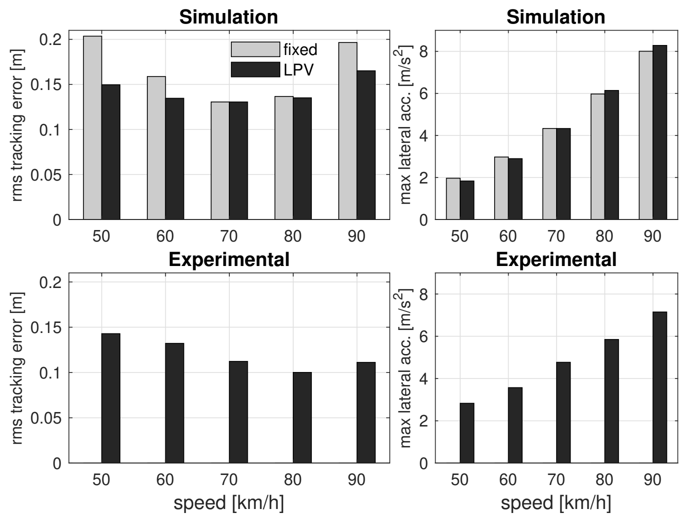

Fig. 14. Tracking RMS error (left) and maximum lateral acceleration (right) for the simulated (top) and experimental (bottom) DLC manoeuvre.

controller, time domain plots for the DLC at 90km/h are provided in Figure 15. In this test, the maximum tracking error is always less than 0.3 m (and in general, never higher than 0.6 m also for different speed values). As side comment, it is worthy to highlight that the controller – designed using a linear vehicle model – proves robust enough to achieve good tracking performances also in the proposed scenario, where a lateral acceleration of 0.8 g and a sideslip angle of 2.5° indicate proximity to the tire saturation condition.

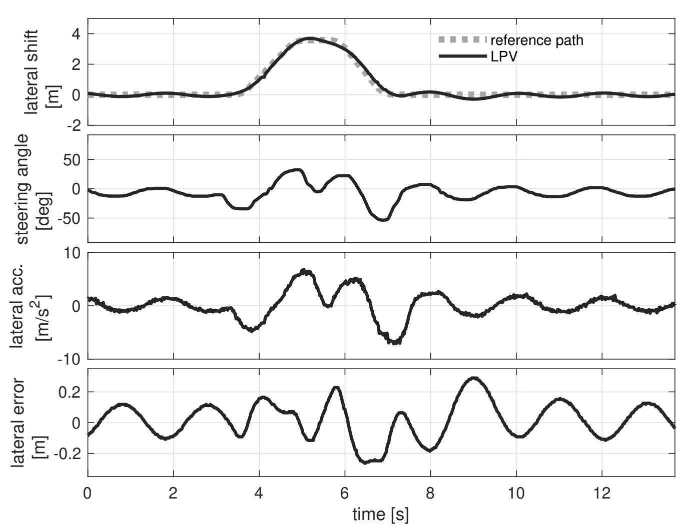

Fig. 15. LPV controller behaviour on the DLC manoeuvrer at 90 km/h.

VI. CONCLUSIONS

The paper discusses the design, implementation and validation of a trajectory tracking system for autonomous cars. The main focus is on guaranteeing adequate tracking performance also in case of aggressive manoeuvres, considering steering actuator nonlinearities, relevant also for non-prototypal vehicles, and possibly varying vehicle speed. This objective is reached without introducing optimization based controllers

The solution consists in the LPV extension of a Multiple Input Single Output Linear Parameter Varying (MIMO-LPV) controller, proposed in [22], that makes possible to consider the objective of controlling both the lateral error at the centre of gravity and its derivative at the look-ahead distance. This yields the ability of performing aggressive manoeuvres as well as steady state cornering with small tracking errors.

The LPV nature is useful to systematically account for the vehicle dynamics dependence on the longitudinal velocity and also the nonlinearities in the steering actuators. The paper provides a detailed discussion of the steering actuator model and the limit cycle that stems from the friction and backlash in the actuator. From a purely control system design point of view, the issue can be addressed by scheduling the bandwidth of the controller according to the curvature. The scheduling shifts the limit cycle to amplitudes and frequencies that are not uncomfortable for the passengers when accurate tracking is not necessary.

Detailed experimental validation on an instrumented vehicle, against three different types of manoeuvres (straight driving, bends and double lane change) proves that the controller can successfully negotiate the manoeuvres with a tracking error of less than 40 cm even in cases with a lateral acceleration of 0.8 g. This performance is deemed adeguate for an autonomous driving scenario. Controller parameters and general guidelines on their tuning are given, so to encourage scientific comparison and practical employment.

In conclusion, the paper shows that adeguate tracking performance can be achieved in a realistic and challenging setting without using optimization based controllers with their burden of complexity and computational demands

Future work will focus on the generation of a feasible trajectory for efficient, safe and stable obstacle avoidance.

REFERENCES

[1] D. González, J. Pérez, V. Milanés, and F. Nashashibi, "A review of motion planning techniques for automated vehicles," *IEEE Transactions on Intelligent Transportation Systems*, vol. 17, no. 4, pp. 1135–1145, 2016.

[2] A. Broggi, M. Buzzoni, S. Debattisti, P. Grisleri, M. C. Laghi, P. Medici, and P. Versari, "Extensive tests of autonomous driving technologies," *IEEE Transactions on Intelligent Transportation Systems*, vol. 14, no. 3, pp. 1403–1415, Sept 2013.

[3] C. Katrakazas, M. Quddus, W.-H. Chen, and L. Deka, "Real-time motion planning methods for autonomous on-road driving: state-of-the-art and future research directions," *Transportation Research Part C: Emerging Technologies*, vol. 60, pp. 416–442, 2015.

[4] D. Ferguson, T. M. Howard, and M. Likhachev, "Motion planning in urban environments," *Journal of Field Robotics*, vol. 25, no. 11-12, pp. 939–960, 2008.

[5] J. Guldner, V. Utkin, J. Ackermann *et al.*, "A sliding mode control approach to automatic car steering," in *American Control Conference, 1994*, vol. 2. IEEE, 1994, pp. 1969–1973.

[6] M. Schorn, U. Stählin, A. Khanafer, and R. Isermann, "Nonlinear trajectory following control for automatic steering of a collision avoiding vehicle," in *American Control Conference, 2006*. IEEE, 2006, pp. 6–pp.

[7] S. C. Peters, E. Frazzoli, and K. Iagnemma, "Differential flatness of a front-steered vehicle with tire force control," in *Intelligent Robots and Systems (IROS), 2011 IEEE/RSJ International Conference on*. IEEE, 2011, pp. 298–304.

[8] J. C. Gerdes and E. J. Rossetter, "A unified approach to driver assistance systems based on artificial potential fields," *Journal of Dynamic Systems, Measurement, and Control*, vol. 123, no. 3, pp. 431–438, 2001.

[9] E. J. Rossetter, J. P. Switkes, and J. C. Gerdes, "Experimental validation of the potential field lanekeeping system," *International journal of automotive technology*, vol. 5, no. 2, pp. 95–108, 2004.

[10] Kritayakirana, "Autonomous vehicle control at the limits of handling," Ph.D. dissertation, Stanford, 2012.

[11] C. E. Beal and J. C. Gerdes, "Model predictive control for vehicle stabilization at the limits of handling," *Control Systems Technology, IEEE Transactions on*, vol. 21, no. 4, pp. 1258–1269, 2013.

[12] P. Falcone, F. Borrelli, J. Asgari, H. E. Tseng, and D. Hrovat, "Predictive active steering control for autonomous vehicle systems," *Control Systems Technology, IEEE Transactions on*, vol. 15, no. 3, pp. 566–580, 2007.

[13] F. Borrelli, P. Falcone, T. Keviczky, J. Asgari, and D. Hrovat, "MPC-based approach to active steering for autonomous vehicle systems," *International Journal of Vehicle Autonomous Systems*, vol. 3, no. 2-4, pp. 265–291, 2005.

[14] J. Liu, P. Jayakumar, J. L. Stein, and T. Ersal, "Combined speed and steering control in high-speed autonomous ground vehicles for obstacle avoidance using model predictive control," *IEEE Transactions on Vehicular Technology*, vol. 66, no. 10, pp. 8746–8763, Oct 2017.

[15] R. Sharp, D. Casanova, and P. Symonds, "A mathematical model for driver steering control, with design, tuning and performance results," *Vehicle System Dynamics*, vol. 33, no. 5, pp. 289–326, 2000.

[16] M. Thommyppillai, S. Evangelou, and R. Sharp, "Car driving at the limit by adaptive linear optimal preview control," *Vehicle system dynamics*, vol. 47, no. 12, pp. 1535–1550, 2009.

[17] N. R. Kapania and J. C. Gerdes, "Design of a feedback-feedforward steering controller for accurate path tracking and stability at the limits of handling," *Vehicle System Dynamics*, vol. 53, no. 12, pp. 1687–1704, 2015.

[18] P. Yih and J. C. Gerdes, "Modification of vehicle handling characteristics via steer-by-wire," *IEEE transactions on control systems technology*, vol. 13, no. 6, pp. 965–976, 2005.

[19] X. Huang, H. Zhang, G. Zhang, and J. Wang, "Robust weighted gain-scheduling H_∞ vehicle lateral motion control with considerations of steering system backlash-type hysteresis," *IEEE Transactions on Control Systems Technology*, vol. 22, no. 5, pp. 1740–1753, 2014.

[20] F. Wu, "Control of Linear Parameter Varying systems," Ph.D. dissertation, Mechanical Engineering, University of California, Berkeley, USA, 1995.

[21] P. Gahinet, P. Apkarian, and M. Chilali, "Affine parameter-dependent Lyapunov functions and real parametric uncertainty," *IEEE Transactions on Automatic Control*, vol. 41, no. 3, pp. 436–442, 1996.

[22] F. Roselli, M. Corno, S. Savaresi, M. Giorelli, D. Azzolini, A. Irilli, and G. Panzani, "H^∞ control with look-ahead for lane keeping in autonomous vehicles," in *Control Technology and Applications (CCTA), 2017 IEEE Conference on*. IEEE, 2017, pp. 2220–2225.

[23] "Torc robotics," https://torc.ai/.

[24] Z. Sun, J. Zheng, Z. Man, and H. Wang, "Robust control of a vehicle steer-by-wire system using adaptive sliding mode," *IEEE Transactions on Industrial Electronics*, vol. 63, no. 4, pp. 2251–2262, 2015.

[25] G. Panzani, M. Corno, and S. M. Savaresi, "On adaptive electronic throttle control for sport motorcycles," *Control Engineering Practice*, vol. 21, no. 1, pp. 42–53, 2013.

[26] R. Rajamani, *Vehicle dynamics and control*. Springer Science & Business Media, 2011.

[27] J. Guldner, H.-S. Tan, and S. Patwardhan, *On fundamental issues of vehicle steering control for highway automation*. California PATH Program, Institute of Transportation Studies, University of California, Berkeley, 1997.

[28] P. Hingwe and M. Tomizuka, "A variable look-ahead controller for lateral guidance of four wheeled vehicles," in *American Control Conference, 1998. Proceedings of the 1998*, vol. 1. IEEE, 1998, pp. 31–35.

[29] P. Apkarian, J.-M. Biannic, and P. Gahinet, "Self-scheduled H-infinity control of missile via linear matrix inequalities," *Journal of Guidance, Control, and Dynamics*, vol. 18, no. 3, pp. 532–538, 1995.

[30] F. Wu, K. M. Grigoriadis, and A. Packard, "Anti-windup controller design using linear parameter-varying control methods," *International Journal of Control*, vol. 73, no. 12, pp. 1104–1114, 2000.